Pergamon

Tetrahedron 57 (2001) 5597–5606

TETRAHEDRON

A theoretical study of the selectivity for the domino [5+2]/[4+2] cycloadditions of γ-pyrones bearing tethered alkenes with substituted 1,3-butadienes

Luis R. Domingo[a,*] and Ramón J. Zaragozá[b]

[a]*Instituto de Ciencia Molecular, Universidad de Valencia, Dr Moliner 50, 46100—Burjassot, Valencia, Spain*
[b]*Departamento de Química Orgánica, Universidad de Valencia, Dr Moliner 50, 46100—Burjassot, Valencia, Spain*

Received 5 February 2001; revised 9 April 2001; accepted 24 April 2001

Abstract—Selectivity of the domino [5+2]/[4+2] cycloaddition reactions of a β-silyloxy-γ-pyrone bearing a tethered alkene with two substituted 1,3-butadienes have been theoretically studied at the B3LYP/6-31G*//AM1 and B3LYP/6-31G* computational levels. Analysis of these results allow explaining the regio, stereo and chemoselectivity observed experimentally at these domino reactions. Selectivity outcome is reproduced by these calculations. © 2001 Elsevier Science Ltd. All rights reserved.

1. Introduction

Domino reactions are processes involving two or more bond-forming transformations that take place under the same reaction conditions without adding additional reagents and catalysts, and in which the subsequent reaction results as a consequence of the functionality formed in the previous step.[1] These sequential reactions are characterized by their great elegance, frequently high stereoselectivity, and the simple manner in which they may be carried out. They allow complex molecules to be constructed in only a few steps.[2]

Domino cycloadditions play a key role in organic syntheses where construction of complex polycyclic structures with an adequate regio and stereochemical control is needed.[1–4] The interest in this subject is shown by numerous recent reviews.[2,5,6]

The intramolecular [5+2] cycloaddition of β-alkoxy-γ-pyrones bearing tethered alkenes for rapidly assembling 8-oxabicyclo[3.2.1]octenone systems have been studied extensively by Wender et al.[7–9] and more recently by Mascareñas et al.[10–12] (see Scheme 1). The dense functionalization of the resulting oxabicycles allows their stereoselective elaboration into a variety of products. Presence of a conjugated double bond prompted Mascareñas et al.[13,14] to examine the ability of these compounds as dienophiles in Diels–Alder reactions. This provides a way to fuse a six-membered ring to the seven-membered carbocycles formed in the first [5+2] cycloaddition. Thus, heating a 1:5 mixture of the γ-pyrone **1** and 2,3-dimethyl-1,3-butadiene, **2**, at 160°C leads to the tricarbocyclic adduct **4** in 81% yield.[13] A similar result is obtained using the diene **3** to give a unique regioisomeric adduct **5**[13] (see Scheme 2). More recently, these authors have studied the [5+2]/[4+2] domino cycloaddition of a γ-pyrone bearing a tethered alkyne **6**, with **2** to give the tricarbocyclic adduct **7** in 93% yield[14] (see Scheme 3). These domino reactions take place with a high selectivity, chemo, regio and stereoselectivity, to obtain mainly an enantiomeric pair of adducts along with the formation of five stereogenic centers.

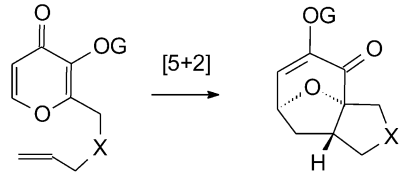

Scheme 1.

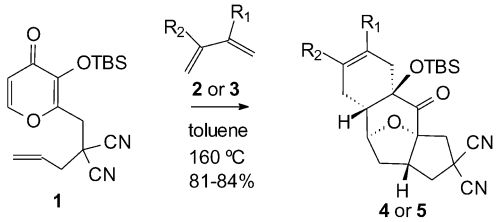

2, 4 R_1=R_2=Me
3, 5 R_1=H, R_2=OTBS

Scheme 2.

Keywords: domino reactions; cycloadditions; mechanisms; selectivity.
* Corresponding author. Fax: +34-96-398-3152;
e-mail: domingo@utopia.uv.es

PII: S0040-4020(01)00464-1

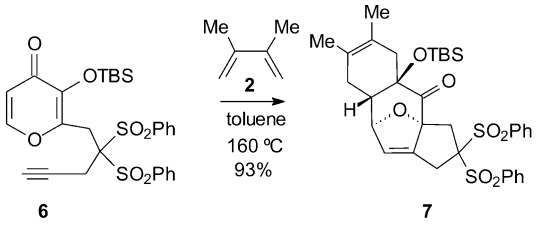

Scheme 3.

it seemed of interest to extend these studies to domino reactions involving different cycloaddition reactions which have neither been treated by computational methods nor any generally accepted molecular mechanism has emerged.

In the present paper, the selectivity for the domino intra [5+2]/inter [4+2] cycloaddition reactions between the γ-pyrone **8** bearing a tethered alkene and the substituted 1,3-butadienes **2** and **13** have been studied as computational

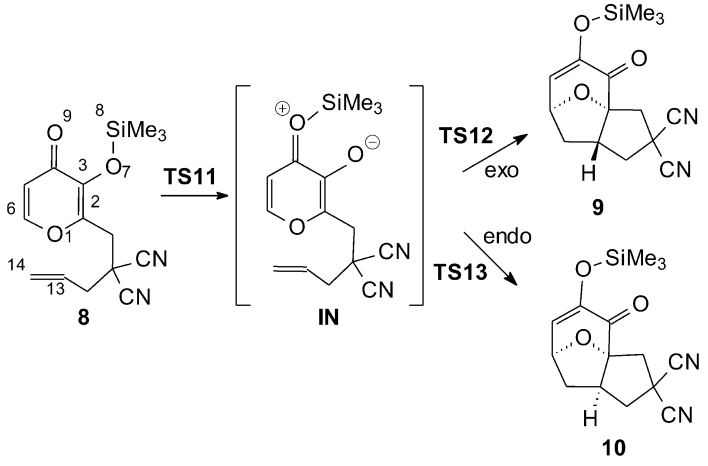

Scheme 4.

Despite the obvious potential of these domino processes and its many variations, the reaction pathways have not been studied theoretically so far. A deep knowledge of the molecular mechanism is fundamental, however, for a rationalization of the experimental results.

Our research program has maintained an interest in these kinds of chemical reactions for long and the understanding of the characteristic feature of these consecutive processes prompted us to explore further the mechanistic aspects. In previous theoretical works, several [4+2]/[4+2][15–18] and [4+2]/[3+2][19,20] domino cycloaddition reactions to give complex polycyclic systems have been studied. Therefore,

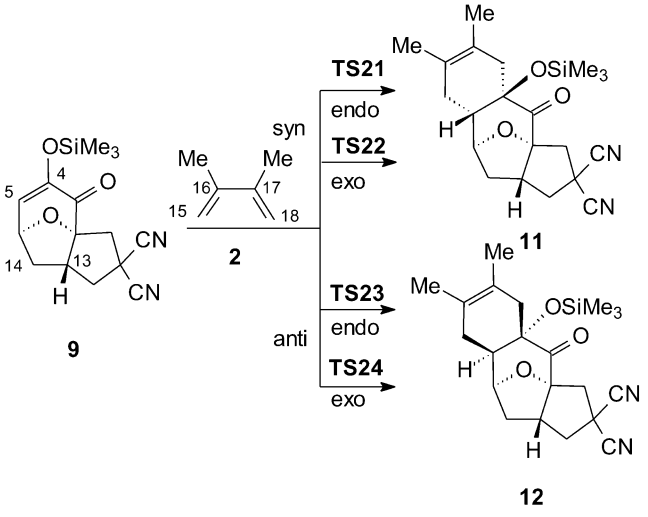

Scheme 5.

models of this type of domino cycloadditions (see Schemes 4–7). An analysis of energetic contributions to the potential energy barriers for the [5+2] and [4+2] cycloadditions identifies different factors controlling the reactive channels. Selectivity outcome is reproduced by these calculations.

2. Computational methods

The potential energy surfaces (PESs) of the domino reactions between **8** and **2**, and **8** and **13**, have been calculated in detail to ensure that all relevant stationary points have been located and properly characterized. All molecular geometries have been fully optimized using the semiempirical AM1 methods[21] implemented in the MOPAC93 package programs.[22] The stationary points along the PES have been located without any geometrical restriction and have been characterized through the calculation of the force constants matrix by ensuring that they correspond to minima or saddle points, i.e. they have zero or one and only one imaginary frequency, respectively. We have used the simplified model **8** instead of the β-silyloxy-γ-pyrone **1**. In Mascareñas's γ-pyrone **1**, the bulky *tert*-butyldimetylsilyl (TBS) group has been replaced for a trimethylsilyl group. Optimized geometries of all structures are available from the authors.

AM1, as other semiempirical methods, has weaknesses, for example in dealing with absolute values of activation energies. Recently, Jursic et al.,[23–26] Oliva et al.[27] and we[17] have shown that the B3LYP/6-31G*//AM1 approach renders qualitatively correct results in studies of related Diels–Alder reactions, and subsequently this computational strategy can be applied in the study of large organic

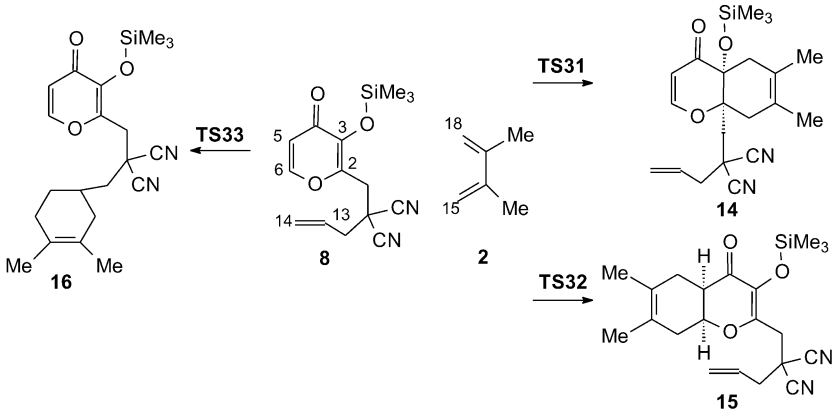

Scheme 6.

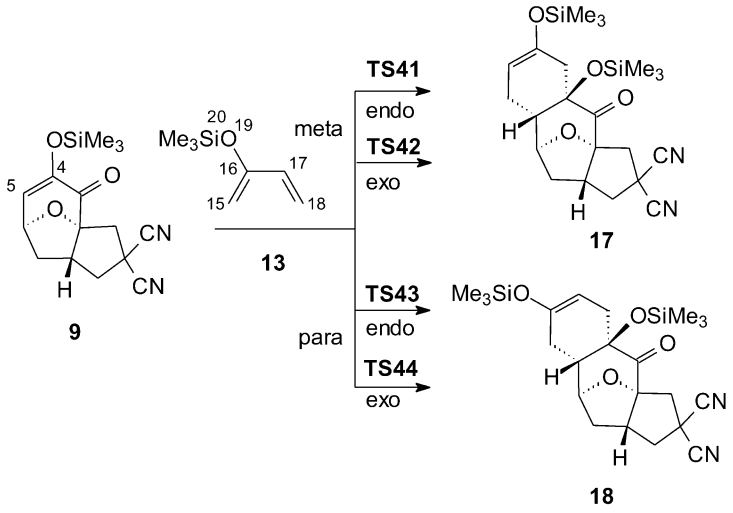

Scheme 7.

molecules.[17,23–27] Consequently, we have used hybrid B3LYP method, this is the gradient corrected functionals of Becke,[28] and Lee et al.,[29] for exchange and non-local correlation, respectively, and the 6-31G* basis set[30] to calculate energetic parameters with the AM1 optimized geometries (B3LYP/6-31G*//AM1 method). Finally, the stationary points corresponding to the domino reaction between **8** and **2** have been optimized completely at B3LYP/6-31G* level in order to assert the capability of this computational approach to study the selectivity of these domino reactions. These calculations have been done using the GAUSSIAN98 program.[31]

3. Results and discussions

The domino reactions between **8** and the 1,3-butadienes **2** or **13** are stepwise processes initialized by the migration of the neighbouring silyl group to the carbonyl group of the γ-pyrone to give a weak oxidopyrylium ylide intermediate **IN**. The subsequent intramolecular [5+2] cycloaddition affords the cycloadduct **9**, which by a consecutive intermolecular [4+2] cycloaddition with **2** or **13** gives the final cycloadducts **11** and **18**, respectively (see Schemes 4, 5 and 7). While the reaction between **8** and **2** presents a clear stereo and π-facial selectivity, the reaction between **8** and **13** has also a total regioselectivity. Moreover, presence of three double bonds on the γ-pyrone **8** opens the possibility for several intermolecular [4+2] cycloadditions with the substituted 1,3-butadienes **2** and **13**.[32] Thus, in order to study the chemoselectivity at this domino reaction we have also considered the intermolecular cycloaddition between **8** and **2** to give the adducts **14**, **15** and **16**, which are not observed (see Scheme 6). Thus, firstly, the intramolecular [5+2] cycloaddition of **8** to give the oxabicyclooctenone **9** is studied (see Scheme 4), and then the intermolecular [4+2] cycloaddition between **9** and **2** (see Scheme 5), and **8** and **2** are considered (see Scheme 6). Finally, the intermolecular [4+2] cycloadditions between **9** and **13** have also been studied (see Scheme 7).

In Schemes 4–7 the stationary points corresponding to the more relevant reactive channels for these domino processes have been presented together with the atom numbering, while the geometries of the TSs are shown in Figs. 1, 2, 4 and 5. The relative energies are summarized in Table 1.

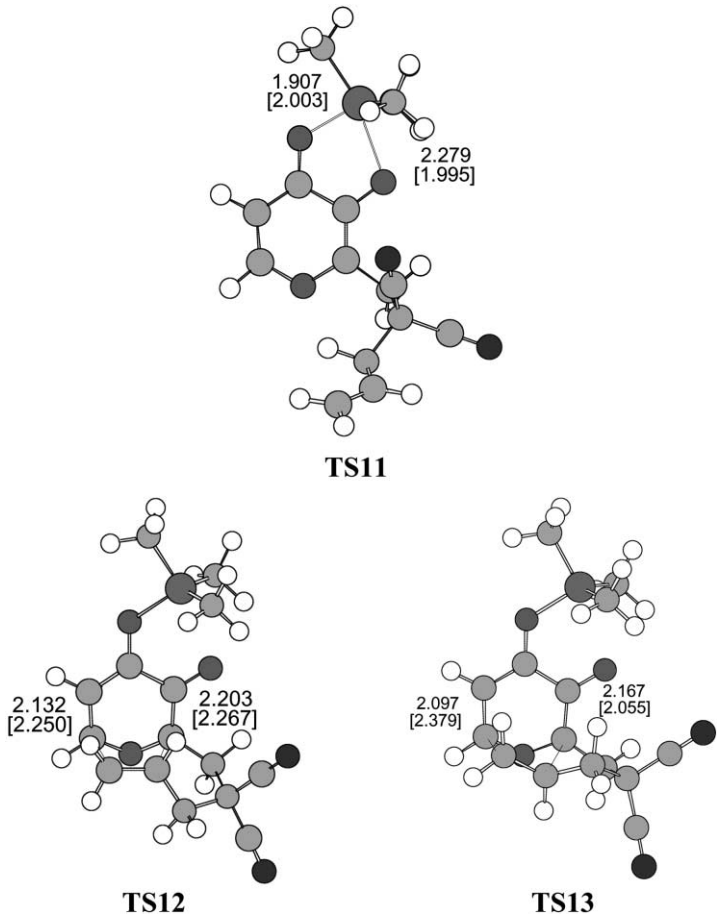

Figure 1. Selected geometrical parameters for the transition structures corresponding to the intramolecular [5+2] cycloaddition of the γ-pyrone **8**. The values of the lengths of the bonds directly involved in the reaction obtained at the AM1 and B3LYP/6-31G* [ ] are given in angstroms.

3.1. Intramolecular [5+2] cycloaddition of 8

Transformation of the β-silyloxy-γ-pyrone **8** into the cycloadduct **9** demands two process: (i) the migration of the trimethylsilyl group from O7 to O9 position, and (ii) an intramolecular [5+2] cycloaddition process (see Scheme 4). Although three reaction modes are possible for this transformation, our recent study for the mechanism of these [5+2] cycloadditions[33] points out that the most favourable reactive channel takes place along a stepwise mechanism which is initialized by the transfer of the trimethylsilyl group with formation of an oxidopyrylium ylide intermediate **IN**. The subsequent intramolecular [5+2] cycloadditions affords the oxabicyclooctenones **9** and **10**. Thus, three TSs, **TS11**, **TS12** and **TS13**, an intermediate, **IN**, and two cycloadducts, **9** and **10**, corresponding to the *endo* and *exo* reactive channels of the [5+2] cycloaddition have been studied. The geometries of the corresponding TSs are shown in Fig. 1.

The first step for the transformation of **8** into **9** or **10** corresponds to the migration of the trimethylsilyl group from the O7 to O9 position, with formation of the oxidopyrylium ylide intermediate **IN**, via the **TS11**. The potential energy barrier (PEB) associated with this process is 10.3 kcal/mol (energetic values correspond to B3LYP/6-31G*//AM1 calculations); formation of the intermediate **IN**, with a similar energy that **TS11**, is very endothermic.[34] In consequence, **IN** is very unstable and with a very low barrier it is quickly converted in **8**.

Due to the free rotation of the chain bearing the tethered alkene, the intermediate **IN** can undergo also two intramolecular [5+2] cycloadditions to give the cycloadducts **9** and **10**, via the **TS12** and **TS13**, respectively. These cycloadditions are related with the *exo* and *endo* approaches of the C13–C14 terminal double bond to the C2 and C6 carbon atoms of intermediate **IN**. The PEBs associated with these [5+2] cycloadditions are 15.5 and 29.6 kcal/mol; the barrier for the transformations of γ-pyrone **8** into the cycloadducts **9** and **10** are 27.1 and 41.2 kcal/mol, respectively. These barriers are very large, and thus explain the high temperature required for this [5+2] cycloaddition reaction.[33] Moreover, the larger PEB associated with **TS13** relative to **TS12**, because of the constrain imposed by the tether along the *endo* approach, is responsible of the total *exo* stereoselectivity found in this intramolecular [5+2] cycloaddition. Formation of the cycloadduct **9** is an exothermic process, −7.4 kcal/mol, whereas formation of the cycloadduct **10** is lightly endothermic, 3.7 kcal/mol. Thus, formation of **10** is kinetic and thermodynamically unfavoured, and justify the unique formation of **9**.[13] The energetic results given in Table 1 show that the B3LYP/6-31G*//AM1 barrier obtained for this intramolecular [5+2] cycloaddition is in complete agreement with that obtained using the B3LYP/6-31G* calculations. Full geometry

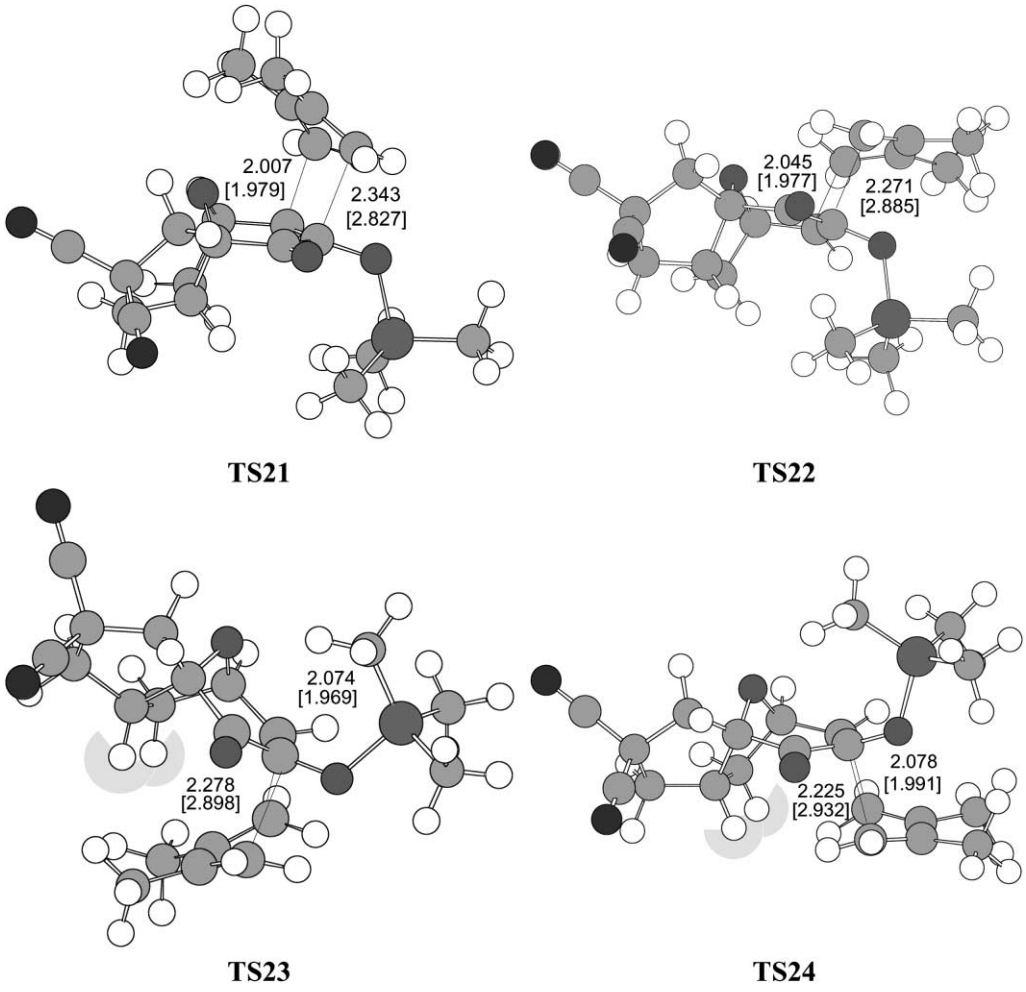

Figure 2. Selected geometrical parameters for the transition structures corresponding to the intermolecular [4+2] cycloaddition of **9** with **2**. **TS23** and **TS24** show the van der Waals radius for the H13 and H14 hydrogens. The values of the lengths of the bonds directly involved in the reaction obtained at the AM1 and B3LYP/6-31G* [ ] are given in angstroms.

optimization at this level gives **IN** 3.1 kcal/mol more stable than **TS11**.

3.2. Intermolecular [4+2] cycloaddition of 9 with 2

The second step for the domino reaction between **8** and 2,3-dimethyl-1,3-butadiene **2** corresponds to the intermolecular [4+2] cycloaddition of the oxabicyclooctenone **9** with **2** (see Scheme 5). This [4+2] cycloaddition can take place along four reactive channels corresponding to the *endo* and *exo* approaches of the substituted 1,3-butadiene **2** to both faces of the conjugated double bond present in **9**, defining the *syn* and the *anti* diasterofacial approach modes. Thus, four TSs have been considered, **TS21** (*endo*/*syn*), **TS22** (*exo*/*syn*), **TS23** (*endo*/*anti*) and **TS24** (*exo*/*anti*), with formation of two final tricarbocyclic adducts, **11** and **12**. The geometries of the corresponding TSs are shown in Fig. 2.

The PEBs associated with the *syn* approach modes are: 23.3 kcal/mol (*endo* **TS21**) and 24.7 kcal/mol (*exo* **TS22**), while the PEBs associated with the *anti* approach modes are 34.4 kcal/mol (*endo* **TS23**) and 35.4 kcal/mol (*exo* **TS24**). These data indicate that both *endo* and *exo* approaches present similar relative energies, the *endo* TS for the more favourable *syn* approaches being 0.4 kcal/mol less energetic than the *exo* one. Along the *syn* and *anti* reactive channels, both *endo* and *exo* approaches give the same cycloadducts. The reaction presents large diasterofacial selectivity, the *syn* approaches are between 10 and 12 kcal/mol more favourable than *anti* ones. Formation of tricarbocyclic adducts **11** and **12** are exothermic processes, ca. −20 kcal/mol (ca. −28 kcal/mol relative to **8** and **2**). These energetic results are in complete agreement with the experimental outcome and explain the formation of the tricarbocyclic adduct **11**.[13]

Finally, the four TSs have been optimized fully at the B3LYP/6-31G* computational level in order to test the *endo* and *syn* diasterofacial selectivities. The PEBs for the [4+2] cycloadditions obtained at the B3LYP/6-31G* level are ca. 5–6 kcal/mol lower than those obtained using the B3LYP/6-31G*//AM1 approach. However, similar *endo* and *syn* diasterofacial selectivities are found at this computational level; the *exo*/*syn* **TS22** is 1.0 kcal/mol more energetic than the *endo*/*syn* **TS21**, and the *endo*/*anti* **TS23** is 9.9 kcal/mol more energetic than the *endo*/*syn* **TS21**. The B3LYP/6-31G* energy profiles for the domino [5+2]/[4+2] cycloaddition between γ-pyrone **8** and 2,3-dimethyl-1,3-

Table 1. AM1 ($\Delta E1$), B3LYP/6-31G*//AM1 ($\Delta E2$), and B3LYP/6-31G* ($\Delta E3$) relative energies (kcal/mol) of transition structures, intermedites and products with respect to reactants for the domino reaction between **8** and **2**, and **8** and **13**

	$\Delta E1$	$\Delta E2$	$\Delta E3$
IN	12.6	11.6	12.7
TS11	12.6	10.3	15.8
TS12	31.5	27.1	27.5
TS13	43.5	41.2	39.5
9	−27.9	−7.4	−13.3
10	−3.0	3.7	2.5
TS21	3.3	15.9	5.0
TS22	2.2	17.3	6.0
TS23	9.8	27.0	14.9
TS24	9.3	28.0	16.5
11	−62.2	−28.1	−34.0
12	−61.2	−26.6	−36.8
TS31	39.1	39.8	
TS32	27.9	31.7	
TS33	26.3	29.1	24.8
14	−25.5	−8.6	
15	−41.8	−21.6	
16	−51.7	−33.2	
TS41	4.6	14.8	
TS42	3.8	16.2	
TS43	0.5	8.3	
TS44	1.3	12.4	
TS45	7.0	20.2	
17	−62.6	−33.6	
18	−61.1	−28.8	

Relative to **8**+**2** or **8**+**13**. **2**: 17.2 kcal/mol (AM1), −234.622450 au (B3LYP/6-31G*//AM1), −234.626780 au (B3LYP/6-31G*). **8**: −52.3 kcal/mol (AM1), −1207.064873 au (B3LYP/6-31G*//AM1), −1207.090636 au (B3LYP/6-31G*). **13**: −63.3 kcal/mol (AM1), −639.903533 au (B3LYP/6-31G*//AM1).

butadiene **2** are shown in Fig. 3. These profiles show the *exo* and *syn* selectivities found at the [5+2] and [4+2] cycloadditions, respectively.

The asynchronicities measured for the TSs corresponding to the [4+2] cycloaddition between **9** and **2** (Δr=l(C4–C15)−l(C5–C18), 0.34 for **TS21**, 0.23 for **TS22**, 0.24 for **TS23**, and 0.15 for **TS24**),[18] indicate that these cycloadditions correspond to asynchronous concerted process,

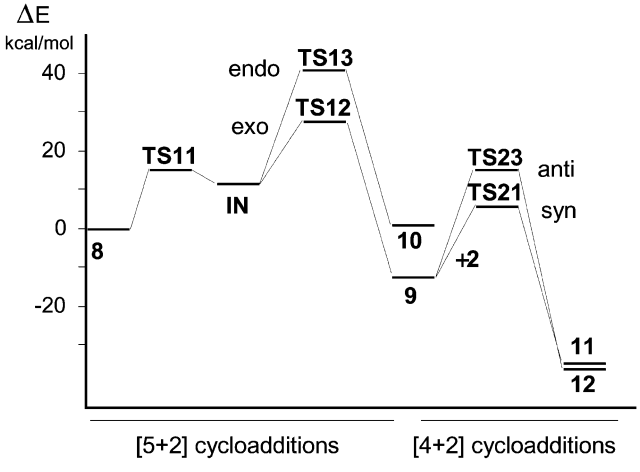

Figure 3. B3LYP/6-31G* Energy profiles for the domino [5+2]/[4+2] cycloaddition reaction between the γ-pyrone **8** and 2,3-dimethyl-1,3-butadiene **2**.

where the C5–C18 forming bonds are more advanced than the C4–C15 ones (these asynchronicities correspond to the AM1 geometries, see Fig. 2). The *syn* approaches are more asynchronous than the *anti* ones. The presence of the conjugated carbonyl group on the dienophile system increases the electrophilic character of the β position of the dienophile fragment, favouring the C5–C18 bond formation. Moreover, an analysis of the geometries corresponding to the *anti* **TS23** and **TS24** shows that both TSs have the H13 and H14 hydrogen atoms in an axial arrangement towards approach of dienophile. Thus, the hindrance that appears along the *anti* approaches may be responsible for the large *syn* diasterofacial selectivity found at these [4+2] cycloadditions (see Fig. 2).[13,14]

B3LYP/6-31G* optimization gives, however, highly asynchronous TSs, Δr are between 0.85 and 0.94. These large values indicate that these cycloadditions are associated with the nucleophilic attack of 1,3-butadiene **2** to the β conjugate position of the α,β-unsaturated carbonyl fragment present on **9** instead of a pericyclic processes. This fact is responsible for the lowering of the B3LYP/6-31G* barriers relative to the AM1 and AM1//B3LYP/6-31G* ones. However, the *endo* and *syn* diasterofacial selectivities for these [4+2] cycloadditions are reproduced at this high computational level.

3.3. Intermolecular [4+2] cycloadditions of 8 with 2

The presence of both 1,3-butadiene **2** and the γ-pyrone **8** in the domino reaction opens the possibility for several intermolecular [4+2] cycloaddition,[32] which are competitive with those corresponding to the reaction of **2** with **9**. Although the corresponding cycloadducts have not been observed experimentally, we have also studied these possibilities in order to understand the origin of the chemoselectivity in this domino reaction. Thus, three TSs, **TS31**, **TS32** and **TS33**, corresponding to the *exo* approaches of the 1,3-butadiene **2** to the C2–C3, C5–C6 and C13–C14 double bonds of the pyrone **8**, with formation of the cycloadducts **14**, **15** and **16**, respectively, have been studied (see Scheme 6). The geometries of the corresponding TSs are shown in Fig. 4.

The PEBs associated with these intermolecular cycloadditions are: 39.8 kcal/mol (**TS31**), 31.7 kcal/mol (**TS32**), and 29.1 kcal/mol (**TS33**). These data show that the intermolecular cycloadditions of 1,3-butadiene **2** with the C2–C3 and the C5–C6 double bonds of the γ-pyrone system have larger barriers than that involving the C13–C14 double bond of the tethered alkene. Although the barrier for the intermolecular [4+2] cycloaddition between **2** and **8** along **TS33** is only 2.0 kcal/mol higher than that of the intermolecular [5+2] cycloaddition of **8** along **TS12**, the inclusion of activation entropy to the activation free energy lies **TS33** ca. 14 kcal/mol above than **TS12**.[33] Moreover, the intermolecular [4+2] cycloaddition between **2** and **8** along **TS33** lies 6 kcal/mol above the intermolecular [4+2] cycloaddition between **2** and **9** along **TS21**. The presence of the C3 carbonyl group in **9** activates the C4–C5 double bond for the reaction with the 1,3-butadiene **2** relative to that with the C13–C14 double bond of **8**. As a result, there is a clear chemoselectivity in this domino reaction; only the

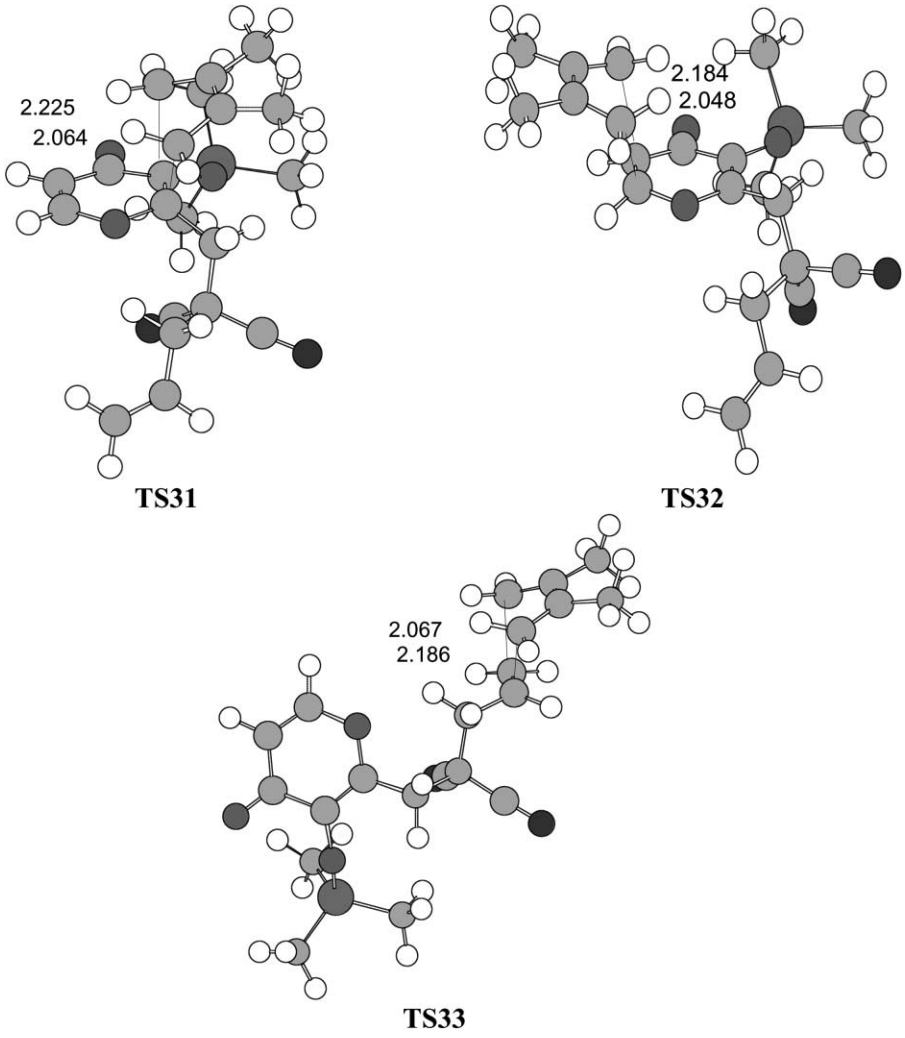

Figure 4. Selected geometrical parameters for the transition structures corresponding to the intermolecular [4+2] cycloaddition of **8** with **2**. The values of the lengths of the bonds directly involved in the reaction obtained at the AM1 are given in angstroms.

[4+2] cycloaddition between **2** and **9** takes place along the intermolecular mode.

Chemoselectivity has been tested by full optimization of the most favourable intermolecular **TS33** at the B3LYP/631G* level. Although these calculations decrease the barrier in ca. 5 kcal/mol, the PEB of **TS33** remains 6.8 kcal/mol higher than that of **TS12**, in agreement with the B3LYP/6-31G*//AM1 results.

3.4. Intermolecular [4+2] cycloaddition of 9 with 13

The second step for the domino reaction between the γ-pyrone **8** and the 2-silyloxy-1,3-butadiene **13** corresponds to the intermolecular [4+2] cycloaddition between **13** and the oxabicyclooctenone **9** (see Scheme 7). Due to the asymmetry present in both reactants this [4+2] cycloaddition can take place along eight reactive channels corresponding to the *endo* and *exo* approaches of the substituted 1,3-butadiene **13** to both faces of the conjugated alkene system present in **9**, defining the *syn* and the *anti* diasterofacial approach modes, and in two regioisomeric possibilities, the *meta* and *para*. However, due to the large *syn* diasterofacial selectivity found in the cycloaddition between **9** and **2**, we have studied only the four *syn* approach possibilities.[35] Thus, four TSs, **TS41** (*endo*/*meta*/*syn*), **TS42** (*exo*/*meta*/*syn*), **TS43** (*endo*/*para*/*syn*) and **TS44** (*exo*/*para*/*syn*), with formation of two final tricarbocyclic adducts **17** and **18** have been considered. The geometries of the corresponding TSs are shown in Fig. 5.

The PEBs associated with the *meta*/*syn* approach modes are: 22.2 kcal/mol (*endo* **TS41**) and 23.6 kcal/mol (*exo* **TS42**), while the PEBs associated with the *para*/*syn* approach modes are 15.7 kcal/mol (*endo* **TS43**) and 19.8 kcal/mol (*exo* **TS44**). The *para* reactive channels are 6.5 kcal/mol more favourable than the *meta* ones. Consequently, B3LYP/6-31G*//AM1 calculations predict a large *para* regioselectivity. Moreover, for the more favourable *para* reactive channels, the *endo* approach is 4.1 kcal/mol less energetic that the *exo* one. Both *endo* and *exo* approaches give the cycloadduct **18**. The presence of the silyloxy group in the 1,3-butadiene system **13** decreases 7.6 kcal/mol the barrier associated with the [4+2] cycloaddition relative to that for the reaction with 2,3-dimethyl-1,3-butadiene **2** via **TS21**. Formation of adducts **17** and **18** are exothermic processes, between −26 and −21 kcal/mol, respectively (−36.6 and −28.8 kcal/mol relative to **8** and **13**). Therefore,

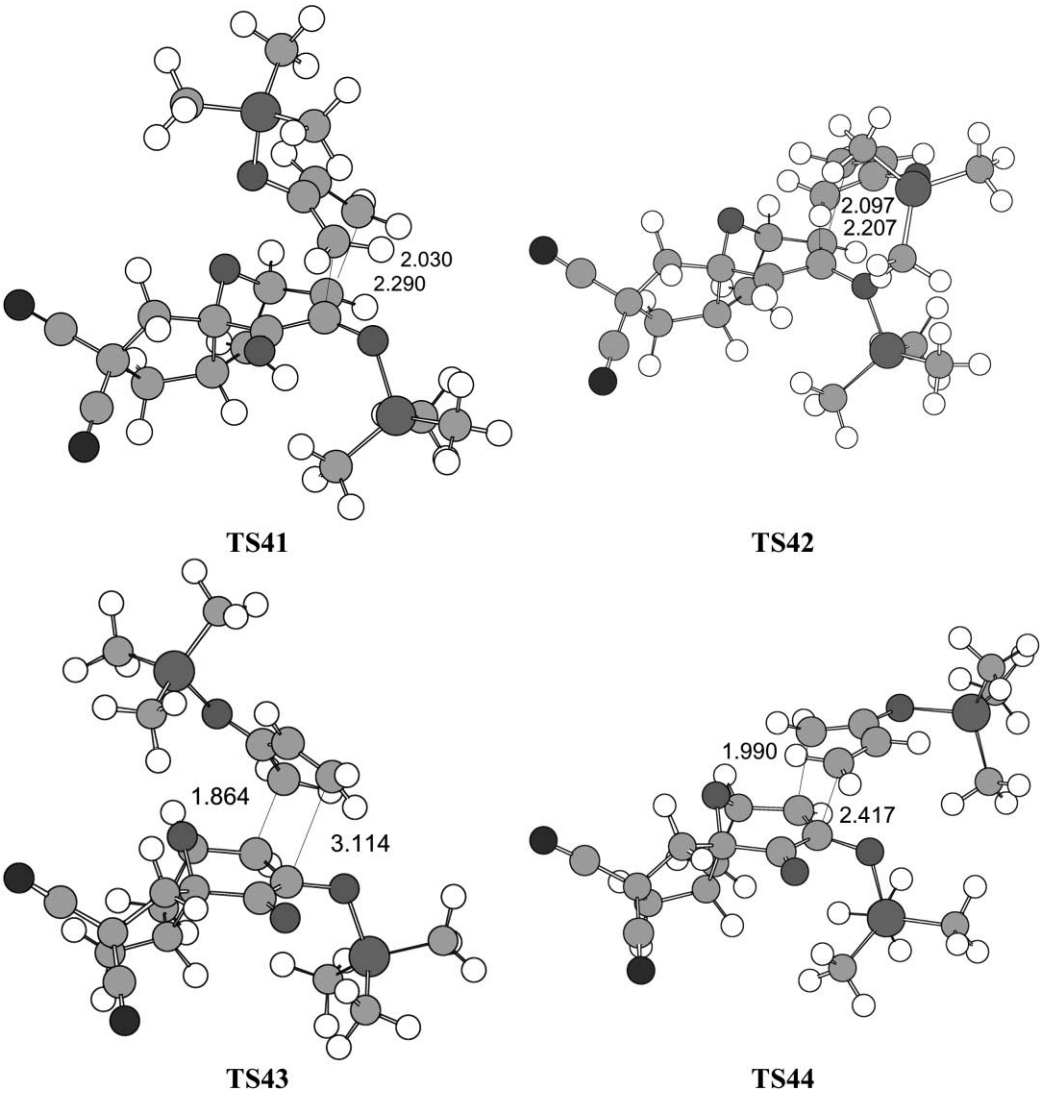

Figure 5. Selected geometrical parameters for the transition structures corresponding to the intermolecular [4+2] cycloaddition of **9** with **13**. The values of the lengths of the bonds directly involved in the reaction obtained at the AM1 are given in angstroms.

formation of the *para* adduct **18** corresponds to the reactive channel of the kinetic control, while formation of the meta adduct **17** corresponds to the cycloadduct of thermodynamic control.[16] These energetic results are in complete agreement with the experimental outcome and allow to explain the formation of the tricarbocyclic adduct **18**.[13]

For the intermolecular [4+2] cycloaddition between **9** and **13**, the asynchronicity measured for the *meta* TSs, Δr=l(C4–C15)−l(C5–C18), are: 0.26 for **TS41**, 0.34 for **TS42**, while for the *para* TSs, Δr=l(C4–C18)−l(C5–C15), are: 1.25 for **TS43** and 0.43 for **TS44**. These data indicate that these cycloadditions correspond to asynchronous processes, where the C5–C*X* (*X*=15 or 18) forming bonds are more advanced than the C4–C*Y* (*Y*=18 or 15) ones. The more favourable *para* TSs are more asynchronous than the *meta* ones. Moreover, the large value of the asynchronicity found for the most favourable reactive channel along the *endo*/*para* **TS43**, Δr=1.25, indicates that this TS corresponds to a highly asynchronous bond-formation process where predominantly the C5–C15 bond is being formed.[36–38] A separation of ca. 3.1 Å at one end of the TS and 1.8 Å at the other leads to appreciable covalent interaction only at the C5 and C15 sites.[34,35]

At the *endo*/*para* **TS43**, the trimethylsilyl ether group adopts a planar arrangement, the C15–C16–O19–Si20 dihedral angle is −173°. This allows a favourable delocalisation of the O19 lone pair on the C15–C16 double bond increasing the nucleophilic character of the 1,3-butadiene.[19,20,37] However, along the *endo*/*meta* approach the 1,3-butadiene **13** behaves as a diene rather than a nucleophile, and the hindrance that appears between the bulky trimethyl silyl group and the bridged O1 oxygen atom is responsible of the non-periplanar arrangement of the silyl group (see **TS43** and **TS41** in Fig. 5).[20]

4. Conclusions

The selectivity for the domino [5+2]/[4+2] cycloaddition reactions of the β-silyloxy-γ-pyrone **8** bearing a tethered alkene with two substituted 1,3-butadienes: 2,3-dimethyl-1,3-butadiene **2**, or 2-trimethylsilyloxy-1,3-butadiene **13**,

has been studied theoretically using the B3LYP/6-31G*//AM1 and B3LYP/6-31G* calculations. The different reaction pathways have been mapped out and TSs, intermediates and cycloadducts have been located and properly characterized. Within the limitation of the B3LYP/6-31G*//AM1 approach, the results give a qualitative picture of these complex domino reactions. These energetic results are in complete agreement with the experimental outcome, and they are able to explain the origin of the selectivities. We can conclude that the correct behaviours of the systems under investigation are reproduced. Full optimization at the B3LYP/6-31G* computational level of the stationary points that control the different selectivities allow us to assert the analysis obtained using the B3LYP/6-31G*//AM1 approach.

These domino processes comprise two consecutive cycloaddition reactions: the first intramolecular [5+2] cycloaddition is initiated by the transfer of the trimethylsilyl group from the O7 to the O9 position of the β-silyloxy-γ-pyrone **8**, with formation of a weak oxidopyrylium ylide intermediate **IN**, which by a subsequent intramolecular [5+2] cycloaddition affords the relatively complex 8-oxabicyclooctane adduct **9**. The second process corresponds to [4+2] intermolecular cycloadditions of this cycloadduct with the substituted 1,3-butadienes **2** or **13**, to give the final tricarbocyclic adducts **11** or **18**, respectively.

For the [5+2] cycloaddition, the constraint imposed by the tether along the *endo* approach is responsible for the large *exo* stereoselectivity found for this type of intramolecular cycloadditions. The [4+2] cycloadditions present a large *syn* diasterofacial selectivity due to hindrance that appears along the *anti* approach. Presence of the silyloxy group on the 1,3-butadiene **13** increases notably the rate of the second cycloaddition along the *endo*/*para* approach; the cycloaddition being very regioselective. Finally, the large activation entropy associated with the intermolecular cycloaddition modes together with the low activation of the double-bonds present in the γ-pyrone **8** are responsible for the chemoselectivity found in these domino reactions. These theoretical results are consistent with the experimental outcomes and shed light on the selectivity of the related domino transformations.

Acknowledgements

This work was supported by research funds provided by the Ministerio de Educación y Cultura of the Spanish Government by DGICYT (project PB98-1429). All calculations were performed on a Cray-Silicon Graphics Origin 2000 of the Servicio de Informática de la Universidad de Valencia. We are most indebted to this center for providing the computer capabilities.

References

1. Tietze, L. F. *Chem. Rev.* **1996**, *96*, 115–136.
2. Tietze, L. F.; Beifuss, U. *Angew. Chem., Int. Ed. Engl.* **1993**, *32*, 131–163.
3. Tietze, L. F.; Haunert, F. Domino Reactions in Organic Synthesis. An Approach to Efficiency, Elegance, Ecological Benefit, Economic Advantage and Preservation of our Resources in Chemical Transformations. In *Stimulating Concepts in Chemistry*; Shibasaki, M., Stoddart, J. F., Voegtle, F., Eds.; Wiley VCH: Weinheim, 2000; pp 39–64.
4. Carruthers, W. *Cycloaddition Reactions in Organic Synthesis*; Pergamon: Oxford, 1990.
5. Denmark, S. E.; Thorarensen, A. *Chem. Rev.* **1996**, *96*, 137–165.
6. Winkler, J. D. *Chem. Rev.* **1996**, *96*, 167–176.
7. Wender, P. A.; McDonald, F. E. *J. Am. Chem. Soc.* **1990**, *112*, 4956–4958.
8. Wender, P. A.; Mascareñas, J. L. *J. Org. Chem.* **1991**, *56*, 6267–6269.
9. Wender, P. A.; Mascareñas, J. L. *Tetrahedron Lett.* **1992**, *33*, 2115–2118.
10. Rumbo, A.; Castedo, L.; Mouriño, A.; Mascareñas, J. L. *J. Org. Chem.* **1993**, *58*, 5585–5586.
11. Mascareñas, J. L.; Rumbo, A.; Castedo, L. *J. Org. Chem.* **1997**, *62*, 8620–8621.
12. Rodríguez, J. R.; Rumbo, A.; Castedo, L.; Mascareñas, J. L. *J. Org. Chem.* **1999**, *64*, 4560–4563.
13. Rodríguez, J. R.; Rumbo, A.; Castedo, L.; Mascareñas, J. L. *J. Org. Chem.* **1999**, *64*, 966–970.
14. Rodríguez, J. R.; Castedo, L.; Mascareñas, J. L. *J. Org. Chem.* **2000**, *65*, 2528–2531.
15. Domingo, L. R.; Arnó, M.; Andrés, J. *Tetrahedron Lett.* **1996**, *37*, 7573–7576.
16. Domingo, L. R.; Arnó, M.; Andrés, J. *J. Am. Chem. Soc.* **1998**, *120*, 1617–1618.
17. Domingo, L. R.; Picher, M. T.; Andrés, J.; Oliva, M. *J. Org. Chem.* **1999**, *64*, 3026–3033.
18. Domingo, L. R.; Picher, M. T.; Andrés, J. *J. Org. Chem.* **2000**, *65*, 3473–3477.
19. Domingo, L. R.; Asensio, A. *J. Org. Chem.* **2000**, *65*, 1076–1083.
20. Domingo, L. R. *Theor. Chem. Acc.* **2000**, *104*, 240–246.
21. Dewar, M. J. S.; Zoebisch, E. G.; Healy, E. F.; Stewart, J. J. P. *J. Am. Chem. Soc.* **1985**, *107*, 3902–3909.
22. Stewart, J. J. P. Fujitsu corp. Ltd., Tokyo, 1993.
23. Jursic, B. S. *J. Mol. Struct. (Theochem)* **1995**, *358*, 139–143.
24. Jursic, B. S. *J. Mol. Struct. (Theochem)* **1996**, *365*, 55–61.
25. Jursic, B. S. *J. Mol. Struct. (Theochem)* **1996**, *379*, 85–91.
26. Jursic, B. S. *J. Mol. Struct. (Theochem)* **1998**, *423*, 189–194.
27. Sbai, A.; Branchadell, V.; Ortuño, R. M.; Oliva, A. *J. Org. Chem.* **1997**, *62*, 3049–3054.
28. Becke, A. D. *J. Chem. Phys.* **1993**, *98*, 5648–5652.
29. Lee, C.; Yang, W.; Parr, R. G. *Phys. Rev. B* **1988**, *37*, 785–789.
30. Hehre, W. J.; Radom, L.; Schleyer, P. v. R.; Pople, J. A. *Ab initio Molecular Orbital Theory*; Wiley: New York, 1986.
31. Frisch, M. J.; Trucks, G. W.; Schlegel, H. B.; Scuseria, G. E.; Robb, M. A.; Cheeseman, J. R.; Zakrzewski, V. G.; Montgomery, J. J. A.; Stratmann, R. E.; Burant, J. C.; Dapprich, S.; Millam, J. M.; Daniels, A. D.; Kudin, K. N.; Strain, M. C.; Farkas, O.; Tomasi, J.; Barone, V.; Cossi, M.; Cammi, R.; Mennucci, B.; Pomelli, C.; Adamo, C.; Clifford, S.; Ochterski, J.; Petersson, G. A.; Ayala, P. Y.; Cui, Q.; Morokuma, K.; Malick, D. K.; Rabuck, A. D.; Raghavachari, K.; Foresman, J. B.; Cioslowski, J.; Ortiz, J. V.; Stefanov, B. B.; Liu, G.; Liashenko, A.; Piskorz, P.; Komaromi, I.; Gomperts, R.; Martin, R. L.; Fox, D. J.; Keith, T.; Al-Laham, M. A.; Peng, C. Y.; Nanayakkara, A.; Gonzalez, C.;

Challacombe, M. W.; Gill, P. M.; Johnson, B.; Chen, W.; Wong, M. W.; Andres, J. L.; Gonzalez, C.; Head-Gordon, M.; Replogle, E. S.; Pople, J. A. GAUSSIAN98, Rev A.6 Gaussian, Inc.: Pittsburgh, PA, 1998.

32. Marko, I. E.; Evans, G. R.; Seres, P.; Chelle, I.; Janousek, Z. *Pure Appl. Chem.* **1996**, *68*, 113–122.
33. Domingo, L. R.; Zaragozá, R. J. *J. Org. Chem.* **2000**, *65*, 5480–5486.
34. Although B3LYP/6-31G*//AM1 results given **TS11** 1.3 kcal/mol less energetic than **IN**, full geometrical optimization at B3LYP/6-31G* level gives **IN** less energetic (see Table 1).
35. The *syn* diasterofacial selectivity for the [4+2] cycloaddition between **9** and **13** was confirmed optimizing the most favourable reactive channel along the *anti* approaches. **TS45**, which corresponds to the *endo*/*para*/*anti* reactive channel, is 11.9 kcal/mol more energetic than **TS43** (see Table 1).
36. Domingo, L. R.; Picher, M. T.; Zaragozá, R. J. *J. Org. Chem.* **1998**, *63*, 9183–9189.
37. Domingo, L. R.; Picher, M. T.; Aurell, M. J. *J. Phys. Chem. A* **1999**, *103*, 11425–11430.
38. Domingo, L. R.; Arnó, M.; Andrés, J. *J. Org. Chem.* **1999**, *64*, 5867–5875.